PRESERVE: adding variable flip-angle excitation to TROSY NMR spectroscopy

Bernhard Brutscher

Université Grenoble Alpes, CEA, CNRS, Institut de Biologie Structurale (IBS), 71 avenue des Martyrs, 38044 Grenoble Cedex 9, France

Correspondence to: B. Brutscher (bernhard.brutscher@ibs.fr)

Abstract. We introduce the PRESERVE pulse sequence element, allowing variable flip-angle adjustment in 2D ^{1}H-^{15}N and ^{1}H-^{13}C TROSY-type correlation experiments. PRESERVE-TROSY exploits a remarkable array of up to nine orthogonal polarization-coherence transfer pathways, showcasing the remarkable potential of spin manipulations achievable through the design and optimization of NMR pulse sequences.

1 Introduction

Transverse-relaxation optimized spectroscopy (TROSY), pioneered by Pervushin and co-workers in 1997 (Pervushin et al., 1997) provides a powerful tool for biomolecular NMR studies of proteins (and other macromolecules), in particular at high static magnetic field strengths. The major pulse sequence block of TROSY is the so-called ST2-PT (Pervushin et al., 1998b) or double S^{3}CT (Sørensen et al., 1997) sequence (**Fig. 1A**). Designed for heteronuclear scalar-coupled 2-spin systems (I-S), this sequence effectively transforms single-transition states of spin S ($S^{+}I^{\alpha}$ or $S^{+}I^{\beta}$) into single-transition states of spin I ($I^{+}S^{\alpha}$ or $I^{+}S^{\beta}$). The relaxation properties of the single-transition states are influenced by cross-correlation between the chemical shift anisotropy (CSA) of the transverse (active) spin and the dipolar (DD) interaction between the two spins (Brutscher, 2000; Goldman, 1984). For nuclear spins with sizeable CSA, selection of the narrowest multiplet component by the ST2-PT sequence therefore provides increased spectral resolution. Moreover, under favourable conditions, it also offers improved experimental sensitivity compared to HSQC variants where the passive spin is decoupled during chemical shift evolution, t_1 (**Fig. 1B**). The extent of line narrowing achieved via CSA-DD cross-correlation is magnetic field dependent with maximal efficiency when the two spin interactions exhibit identical strengths (taking into account the projection of the CSA interaction on the I-S vector). However, spin-state selection inherent to TROSY results in a factor of 2 signal loss relative to decoupled HSQC variants. This loss needs to be compensated by the CSA-dipolar cross-correlation induced line narrowing to yield a net sensitivity gain.

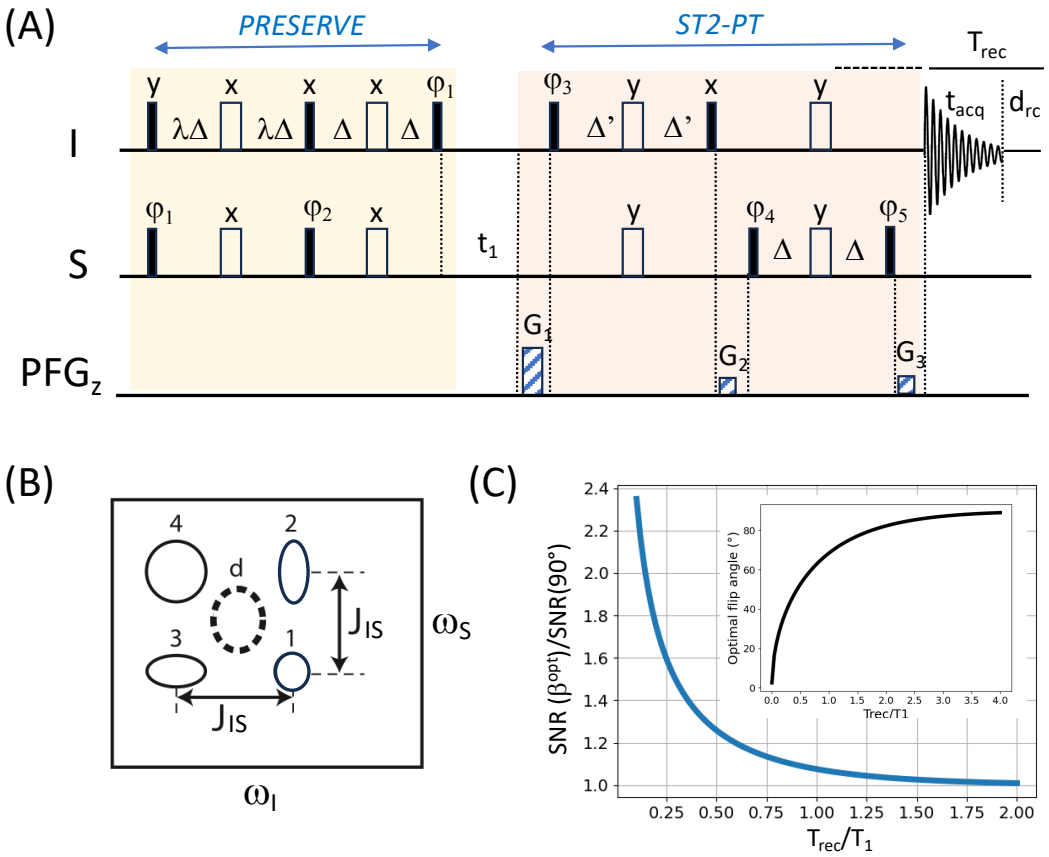

Figure 1. PRESERVE-TROSY experiment for recording heteronuclear 2D I-S correlation spectra. (A) The pulse sequence comprises the PRESERVE, t_1, and ST2-PT building blocks. Filled and open pulse symbols correspond to 90° and 180° rf pulses, respectively. The appropriate single-transition spin-states are selected by adjusting the pulse phases φ_3 and φ_5, as well as the gradients G_1, G_2, and G_3. Echo/anti-echo quadrature detection in t_1 is achieved by the pulsed field gradients G_1, G_2, G_3 with $(G_1\text{-}G_2)/(G_3\text{-}G_2) = \pm \gamma_I/\gamma_S$, and inverting phases φ_3 and φ_5 for the anti-echo component. Phase inversion of the whole PRESERVE sequence by 180° together with the receiver phase improves the line shapes of the detected NMR signals. In addition, axial peak suppression can be realized by inverting phases φ_4 and φ_5 together with the receiver phase. The heteronuclear transfer delay is set to $\Delta = 1/(4J_{IS})$, while Δ' should be chosen slightly shorter in order to reduce the intensity of residual anti-TROSY components.(Schulte-Herbrüggen and Sørensen, 2000) **Small flip angle (β) excitation of I and S spin polarization is achieved by tuning the scaling factor λ to $\lambda = \beta/90°$. (B) Multiplet structure of NMR peaks detected in a scalar coupled I-S spin system, corresponding to the individual single-transition states of the I- and S-spins. This multiplet pattern can be reduced to a single peak using either heteronuclear spin decoupling (HSQC: peak d) or spin-state selection (TROSY: either one of the 4 peaks). (C) Numerical simulation of the expected sensitivity gain if an optimal flip angle is chosen instead of the common 90° nutation, as a function of the T_{rec}/T_1 ratio. The plot in the insert shows the computed optimal flip angle as a function of the T_{rec}/T_1 ratio according to equation (1). These simulations neglect spin relaxation and pulse imperfections.**

The ST2-PT sequence, and thus the TROSY experiment, has some particularly interesting features. First, it allows for sensitivity-enhanced quadrature detection that means that both of the orthogonal S-spin components S_x, S_y (and $2S_xI_z$, $2S_yI_z$), present after a free evolution delay t_1, are transferred into detectable antiphase (or in-phase) coherence $2I_xS_z$, $2I_yS_z$ (I_x, I_y) in a so-called echo/antiecho detection mode (Kay et al., 1994; Palmer et al., 1992; Weigelt, 1998). Second, as the single-transition operators, $S_xI^\alpha = (S_x + 2S_xI_z)/2$ and $S_xI^\beta = (S_x - 2S_xI_z)/2$ are linear combinations of the Cartesian spin

operators S_x and $2S_xI_z$, the equilibrium polarization of the two spin reservoirs (I and S) can be exploited via two parallel polarization-coherence-transfer pathways, where spin polarization of S (S_z) is transferred into S_x in-phase coherence, while spin polarization of I (I_z) is transferred into $2S_xI_z$ antiphase coherence, or *vice versa*, using for example an INEPT-type sequence (Brutscher et al., 1998; Pervushin et al., 1998a). Finally, I-spin polarization (I_z) that is building up during t_1 via longitudinal spin relaxation processes is converted by the ST2-PT sequence into S-spin polarization (S_z) that contributes to the detected NMR signal during the subsequent scan (pulse sequence repetition) (Favier and Brutscher, 2011). This last feature is particularly interesting in the context of BEST-TROSY (Farjon et al., 2009; Favier and Brutscher, 2011; Solyom et al., 2013) where short interscan delays are employed, thus minimizing relaxation-induced losses of the "over-polarized" (higher than thermally polarized) S-spins. Therefore, in total five complementary orthogonal coherence transfer pathways contribute to the detected signal in TROSY and BEST-TROSY-type experiments.

In order to make TROSY experiments even more versatile, it would be appealing to implement the option of variable flip angle excitation to further increase the steady-state spin polarization at high repetition rates. The concept of using non-90° nutation angles (β) as a mean of maximizing the sensitivity in a single-pulse experiment goes back to Richard Ernst and the early days of Fourier transform NMR (Ernst and Anderson, 1966). The nutation angle β^{opt} providing the highest sensitivity is usually called the Ernst angle and it can be shown that for the simple case of a NMR experiment consisting of a single excitation rf pulse followed by signal detection and a recovery period (recycle delay) it fulfils the relation

$$cos\beta^{\mathrm{opt}} = \exp(-T_{rec}/T_1), \quad (1)$$

with T_{rec} the spin polarization recovery time (composed of the signal acquisition time, t_{acq}, and the recycle delay d_{rc}) and T_1 the effective longitudinal relaxation time of the excited spins (**Fig. 1C**). Transferring this concept to multi-pulse sequences employing a series of 90° and 180° pulses is a non-trivial task. So far, it has been adapted to HMQC- and HMBC-type heteronuclear correlation experiments that require a single I-spin excitation pulse followed by one or several 180° pulses. In this case, Ernst angle excitation can still be realized by adjusting the nutation flip angle of the initial excitation pulse to $a^{\mathrm{opt}} = \beta^{\mathrm{opt}} + n \times 180°$ with n the number of additional 180° pulses. This has allowed the development of SOFAST-HMQC and its variants (Gal et al., 2007; Kern et al., 2008; Koos and Luy, 2019; Mueller, 2008; Schanda et al., 2005; Schanda and Brutscher, 2005) for fast and sensitive recording of 2D ^{1}H-^{15}N and ^{1}H-^{13}C correlation spectra, as well as NORD NMR spectroscopy (Nagy et al., 2021).

2 PRESERVE-TROSY

Implementing Ernst-angle excitation in TROSY-type experiments is particularly challenging, because, ideally, it requires a pulse sequence that preserves part of the steady state polarization for both the I- and S-spin reservoirs. Nonetheless, we present here a pulse scheme that fulfils this task. In the pulse sequence depicted in **Fig. 1A**, the initial INEPT transfer scheme of a TROSY experiment has been replaced by an alternative building block that we will refer to as

Polarization Restoring Excitation SEquence foR Versatile Experiments (**PRESERVE**). It allows adjustment of the effective excitation flip angle β for both the I and S spin polarizations by setting the scaling factor of the initial transfer delays to $\lambda = \beta/90°$. Of course, only a single effective excitation angle β can be chosen for both the I and S spins, which in case of large differences in longitudinal relaxation efficiency means that it cannot be adjusted to its theoretical optimum value for both spin species simultaneously. The *sin*β part of I and S polarization is then transferred, as usual, to single-quantum S spin coherence, while the remaining *cos*β I_z and *cos*β S_z parts are "preserved" as spin polarization or 2-spin order as will be explained in more detail below. The main coherence transfer pathways of a TROSY experiment that contribute to the detected NMR signal are conserved in this PRESERVE-TROSY experiment with the only difference being that I spin polarization (I_z) is transferred into in-phase coherence ($\pm S_x$), while S spin polarization (S_z) is transferred into antiphase coherence ($\pm 2S_xI_z$) by the PRESERVE pulse sequence element. For proper functioning of this sequence, all pulse phases need to be adjusted carefully in order to ensure that the appropriate coherences (single-transition states) are selected and that all coherence transfer pathways add constructively to the recorded NMR signal. In the following, we will discuss how this can be achieved for ^{1}H-^{15}N and ^{1}H-^{13}C spin systems.

2.1 ^{1}H-^{15}N PRESERVE-TROSY

For ^{1}H-^{15}N spin systems, the lower right cross peak (**Fig. 2C**) benefits from CSA-dipolar cross-correlation-induced line narrowing in both the ω_N and ω_H spectral dimensions. Selection of this multiplet component, often called the TROSY peak, imposes particular phase settings on the ST2-PT pulse sequence block, and the coherence selection gradients (**Fig. 2A**). While there is general consensus on the TROSY peak to be selected and the required phase settings, there are discrepancies in the literature concerning the assignment of this TROSY peak to the corresponding single-transition spin states. This may be due to different definitions of signs of frequencies and phases, and their translation into actual spin rotations in product operator space (Levitt, 1997; Levitt and Johannessen, 2000). Throughout this manuscript, we will consider that the spectrometer phases are independent of the gyromagnetic ratio (γ) of a given spin species, and thus the same pulse phase induces rotations of opposite sense for nuclear spins with positive or negative γ.

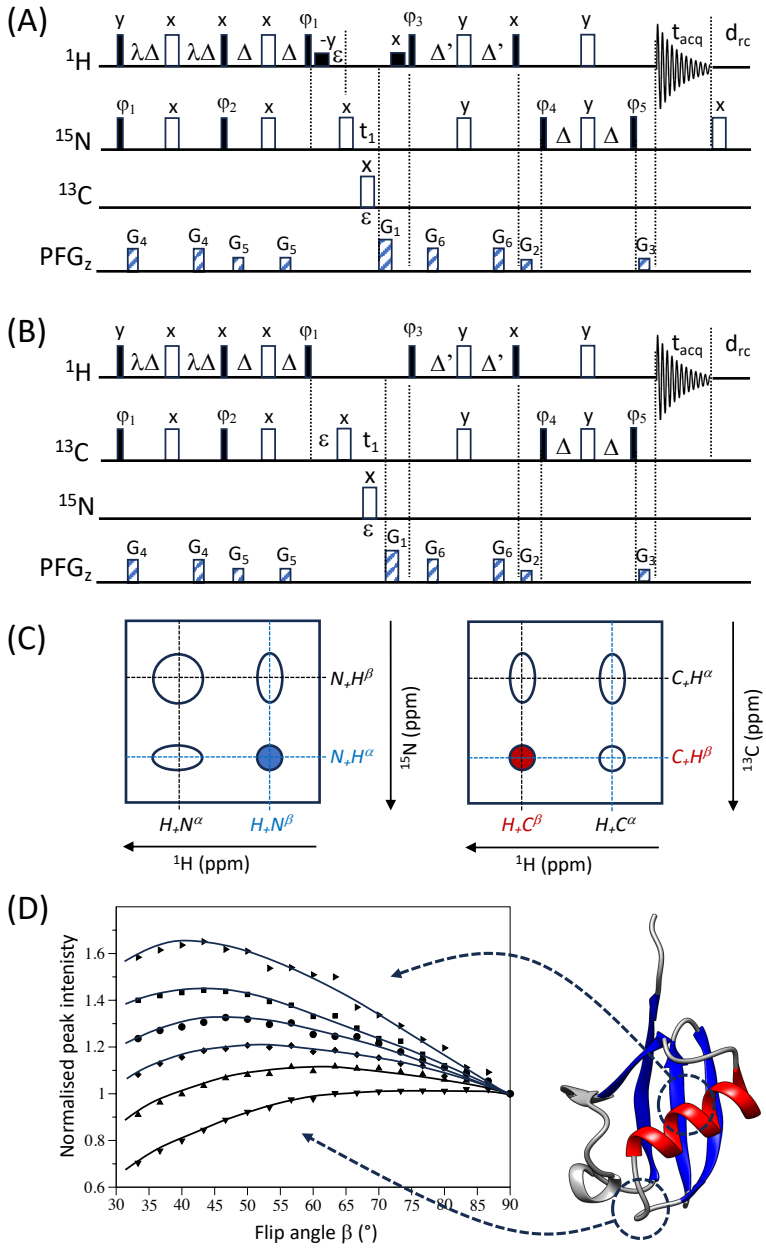

Figure 2. PRESERVE-TROSY pulse sequences for (A) ^{1}H-^{15}N and (B) ^{1}H-^{13}C spin systems. The two pulse sequences differ in the additional 180° pulse after signal detection that is only required for sequence (A) and the initial phase setting for φ_5. In addition, selective ^{1}H 90° pulses (small black squares) are added in the ^{1}H-^{15}N version (A) for water flip-back (WFB) purposes.(Grzesiek and Bax, 1993) **The initial phase settings are: φ_1=x, φ_2=x, φ_3=y, φ_4=x, and φ_5=y (A) and φ_5=-y (B). Phase cycling and quadrature detection is performed as explained in figure 1. (C) Assignment of individual doublet lines in ^{1}H-^{15}N and ^{1}H-^{13}C spectra to the corresponding single-transition spin operators (in accordance with our pulse sequence simulations). The peak selected by sequences (A) and (B) is highlighted in blue (^{1}H-^{15}N) and red (^{1}H-^{13}C). (D) Peak intensities of representative amide groups, extracted from ^{1}H-^{15}N WFB-PRESERVE-TROSY spectra recorded for uniformly ^{2}H/^{13}C/^{15}N-labeled ubiquitin at 25°C, 950 MHz with d_{rc}=0 (T_{rec}=t_{acq}= 70 ms) plotted as a function of the excitation flip angle β. All intensity curves are normalized to 1 for β = 90°. A cartoon structure of ubiquitin is shown in the right panel.**

The ^{1}H-^{15}N version of PRESERVE-TROSY is depicted in **Fig. 2A**. The pulse sequence includes additional water-flip-back pulses to make it applicable to samples in aqueous solution that will not be further discussed in this section. The ^{1}H-^{15}N spin system is characterized by gyromagnetic ratios of opposite sign ($\gamma_H > 0$, $\gamma_N < 0$) and a negative scalar coupling ($J_{NH} < 0$). The ^{1}H- and ^{15}N-spin polarizations are split by the PRESERVE sequence in separate pathways with amplitudes *cos*β and *sin*β, respectively. The *sin*β parts of PRESERVE are the "active" pathways that are detected at the end of the pulse sequence and give rise to the TROSY peak:

$$H_z,\ N_z \xrightarrow{PRESERVE\ (sin\beta)} -H^{\alpha}N_x \xrightarrow{\pi N_x} -H^{\alpha}N_x \xrightarrow{ST2-PT} +H_xN^{\beta}\left(\frac{M_H+M_N}{2}\sin\beta\right) \quad (2)$$

The normalized amplitude, or transfer efficiency, of these two pathways is given in parenthesis at the end, where M_H and M_N correspond to the steady-state magnetizations of ^{1}H and ^{15}N, respectively, and spin-relaxation effects have been neglected. For simplicity, we don't consider here spin evolution during t_1, resulting in similar pathways for the y-components of the single-transition spin operators (Zuiderweg and Rousaki, 2011).

In the following we will concentrate on the additional polarization-coherence transfer pathways that are enabled by PRESERVE if $\lambda < 1$ is chosen for the initial transfer step:

$$H_z \xrightarrow{PRESERVE(\cos\beta)} -2\,H_zN_z \xrightarrow{\pi N_x} +2H_zN_z \xrightarrow{ST2-PT} +H_z\ (M_H\cos\beta) \quad (3)$$

The unused ^{1}H spin polarization is thus stored as H_z during the inter-scan delay similar to a small flip angle single-pulse experiment. The situation becomes a little more complex for the ^{15}N spin polarization that undergoes the following transformations:

$$N_z \xrightarrow{PRESERVE(cos\beta)} -N_z \xrightarrow{\pi N_x} +N_z \xrightarrow{ST2-PT} -2H_zN_z \xrightarrow{\pi N_x} +2H_zN_z\ (M_N\cos\beta) \quad (4)$$

The unused ^{15}N spin polarization is converted into 2-spin order which does not directly contribute to the NMR signal in the subsequent scan, but requires a second reshuffling by the pulse sequence during the next scan:

$$+2H_zN_z\ (M_N\cos\beta) \xrightarrow{PRESERVE} +H_z \xrightarrow{\pi N_x} +H_z \xrightarrow{ST2-PT} -N_z \xrightarrow{\pi N_x} +N_z\ (M_N\cos\beta) \quad (5)$$

The *cos*β part of the ^{15}N spin polarization needs to pass the PRESERVE-TROSY sequence twice before becoming again ^{15}N spin polarization that contributes to the NMR signal of the following scan. Note that an additional 180° ^{15}N pulse is required at the end of the signal detection period in order to make this pulse sequence function properly.

Furthermore, as already described previously (Favier and Brutscher, 2011), ^{1}H polarization that builds up during t_1 due to longitudinal ^{1}H spin relaxation will also be converted by the ST2-PT sequence into ^{15}N polarization, thus contributing to the "active" coherence transfer pathway in the subsequent scan:

$$\ldots \xrightarrow{1H\ spin\ relaxation\ (t1)} +H_z \xrightarrow{ST2-PT} -N_z \xrightarrow{\pi N_x} +N_z \quad (6)$$

In a very similar way, ^{15}N polarization created during t_1 by spin-lattice relaxation is not lost, but will be re-injected as 2-spin order in the following scan:

$$\ldots \xrightarrow{15N\ spin\ relaxation\ (t1)} +N_z \xrightarrow{ST2-PT} -2H_zN_z \xrightarrow{\pi N_x} +2H_zN_z \quad (7)$$

In practice, although conceptually interesting, this last pathway will not contribute significantly to the detected NMR signal because of the low gyromagnetic ratio γ_N ($\gamma_H \approx 10\gamma_N$) and the long longitudinal relaxation times of ^{15}N, especially at high magnetic field strengths.

For echo/antiecho quadrature detection in t_1, the φ_1 phases of the PRESERVE sequence have to be inverted in concert with phases φ_3 and φ_5 of the ST2-PT pulse sequence part. These synchronized phase adjustments preserve the outcomes of the supplementary coherence transfer pathways introduced in Eqs. (3-5).

2.2 ^{1}H-^{13}C PRESERVE-TROSY

For ^{1}H-^{13}C spin systems that are characterized by positive gyromagnetic ratios ($\gamma_H > 0$, $\gamma_C > 0$) and a scalar coupling of positive sign ($J_{CH} > 0$) slightly different phase settings are required. Line narrowing (broadening) of ^{1}H-^{13}C moieties in proteins and nucleic acids can be substantial in the ^{13}C dimension, while only little differences in line width are observed in the ^{1}H dimension at currently available high magnetic field strengths. The line narrowing effect is particularly important for aromatic ^{1}H-^{13}C moieties in protein side chains or nucleic acid bases. Therefore either one of the ^{1}H single-transition spin states (H_xC^α and H_xC^β) may be selected by a TROSY-type experiment (Brutscher et al., 1998). A ^{1}H-^{13}C version of PRESERVE-TROSY is shown in **Fig. 2B** that selects the lower left component of the C-H multiplet (**Fig. 2C**). The polarization-coherence transfer pathways relevant for the ^{1}H-^{13}C PRESERVE-TROSY experiment are as follows:

$$H_z,\ C_z \xrightarrow{PRESERVE\ (sin\beta)} +H^\beta C_x \xrightarrow{\pi C_x} +H^\beta C_x \xrightarrow{ST2-PT} +H_xC^\beta \left(\frac{M_H+M_C}{2}\sin\beta\right) \quad (8)$$

$$H_z \xrightarrow{PRESERVE(\cos\beta)} +2\,H_zC_z \xrightarrow{\pi C_x} -2H_zC_z \xrightarrow{ST2-PT} +H_z\ (M_H\cos\beta) \quad (9)$$

$$C_z \xrightarrow{PRESERVE(cos\beta)} -C_z \xrightarrow{\pi C_x} +C_z \xrightarrow{ST2-PT} -2H_zC_z\ (M_C\cos\beta) \quad (10)$$

$$-2H_zC_z\ (M_C\cos\beta) \xrightarrow{PRESERVE} +H_z \xrightarrow{\pi C_x} +H_z \xrightarrow{ST2-PT} +C_z\ (M_C\cos\beta) \quad (11)$$

$$\ldots \xrightarrow{1H\ spin\ relaxation\ (t1)} +H_z \xrightarrow{ST2-PT} +C_z \quad (12)$$

$$\ldots \xrightarrow{13C\ spin\ relaxation\ (t1)} +C_z \xrightarrow{ST2-PT} -2H_zC_z \quad (13)$$

Again, all polarization-coherence transfer pathways add up in a coherent way, contributing to the detected NMR signal either directly, or after passing the sequence several times. Contrary to the ^{1}H-^{15}N version, no additional 180° ^{13}C pulse is required after the NMR signal detection period.

3 PRESERVE, Ernst angle and experimental sensitivity

The experimental sensitivity of an experiment, defined as the NMR signal recorded in a fixed amount of time (neglecting spin relaxation) is given by :

$$SNR(T_{rec}/T_1, \beta) = \frac{(1-exp(-T_{rec}/T_1)\sin\beta)}{1-\cos\beta exp(-T_{rec}/T_1)\sqrt{T_{rec}+T_{Seq}}} \quad (14)$$

with $T_{rec} = t_{acq} + d_{rc}$ the effective recycle delay, during which spin-lattice relaxation occurs, T_1 the longitudinal relaxation time, and T_{seq} the length of the pulse sequence that does not contribute to the spin polarization build-up. As already indicated above, this function reaches its maximum if $cos\beta^{opt} = \exp(-T_{rec}/T_1)$ $(Eq.(1))$. Therefore a 90° excitation angle is only close to optimal if a recycle delay $T_{rec} > 4T_1$ is chosen (**Fig. 1C**). In all other cases, Eq. (14) predicts a gain in experimental sensitivity if an excitation angle $\beta < 90°$ is chosen. The sensitivity gain achieved with Ernst-angle excitation compared to standard 90° pulse excitation becomes significant in the context of fast-pulsing NMR experiments using recycle delays that are much shorter than the longitudinal relaxation times of the excited spins (**Fig. 1C**). For example, if the recycle delay is 4-times shorter than the longitudinal relaxation time, the expected sensitivity gain amounts to about 60%.

In case of the PRESERVE-TROSY experiment this theoretical sensitivity gain becomes reduced by spin-relaxation-induced signal losses during the different pulse sequence elements (PRESERVE, t_1, ST2-PT) and the recycle delay, as well as by other experimental imperfections, e.g. B_1-field inhomogeneities. Therefore the exact outcome will depend on the particular application (sample, magnetic field strength, spin system, …). In general, the experiment is expected to be most attractive for I-S spin systems characterized by long longitudinal relaxation times for both I and S, and applications aiming at short overall experimental times (short recycle delays).

In order to illustrate this "new" feature of optimizing experimental sensitivity in TROSY experiments at low T_{rec}/T_1 ratios using the PRESERVE sequence element, we have recorded a series of 2D ^{1}H-^{15}N WFB-PRESERVE-TROSY spectra on a triple labelled ($^{13}C/^{15}N/^{2}H$) sample of ubiquitin at high magnetic field strength (950 MHz) and without additional recycle delay ($d_{rc} = 0$). The deuteration of the protein ensures long ^{1}H longitudinal relaxation times for amide protons protected from solvent exchange. Characteristic examples of measured peak intensities for individual amide sites of ubiquitin as a function of the effective excitation flip angle β are shown in **Fig. 2D**. The maxima of these intensity curves are detected at flip angles ranging from about 40° to 90°. This reflects the spread of longitudinal ^{1}H (and evtl. ^{15}N) relaxation times (T_1) in our ubiquitin sample with the shortest T_1 observed for amide groups in the disordered parts (optimal flip angle close to 90°) , and the longest ones in the well-structured parts of the protein (optimal flip angle << 90°). A sensitivity gain of more than 60% is achieved for the amide sites experiencing the slowest ^{1}H longitudinal relaxation. Overall, the sensitivity gains we observe experimentally for optimal flip-angle adjustment are in good agreement with theory (**Fig. 1C**), highlighting the performance of PRESERVE-TROSY to restore "unused" ^{1}H and ^{15}N polarization for subsequent scans.

4 SOFAST-TROSY: combining longitudinal relaxation enhancement with variable flip angle excitation

An alternative approach to enhance the experimental sensitivity in TROSY NMR experiments and to allow for high repetition rates (short inter-scan delays) is the use of longitudinal relaxation enhancement (LRE) techniques (Brutscher and Solyom, 2017; Pervushin et al., 2002; Schanda, 2009). The most prominent and widely used example is arguably the BEST-TROSY implementation. In Band-selective Excitation Short-Transient (BEST) experiments (Schanda et al., 2006), the high-power squared ^{1}H pulse shapes are replaced by amplitude and/or phase modulated pulse shapes that allow excitation of only a subset of ^{1}H spins that are spectrally well separated, while leaving all others (outside this spectral region) close to equilibrium. During the inter-scan delay, the ^{1}H spins in thermal equilibrium then act as a low-energy reservoir that can "absorb" energy from the excited (high energy) ^{1}H via either dipolar relaxation or hydrogen exchange mechanisms.

Although LRE will reduce the interest of variable flip angle excitation, we implemented the PRESERVE building block into a BEST-TROSY experiment that we will refer to as SOFAST-TROSY. **Figure 3** shows different implementations of SOFAST-TROSY, optimized for ^{1}H-^{15}N (Figs. **3A** and **3B**) or ^{1}H-^{13}C (**3C**) spin systems. The ^{1}H-^{15}N SOFAST-TROSY sequences differ in the choice of the band-selective ^{1}H pulse shapes. The version of **Fig. 3A** uses E-BURP2 (Geen and Freeman, 1991) pulse shapes for ^{1}H 90° excitation and flip-back pulses, resulting in a more compact (shorter) pulse sequence, while in the pulse sequence of **Fig. 3B**, symmetric (universal rotation) 90° pulse shapes (PC9) (Kupce and Freeman, 1993) were preferred because of their cleaner excitation profile. In the case of short inter-scan delays, even small perturbations of the "passive" ^{1}H spins can have a significant impact on longitudinal ^{1}H spin relaxation (Schanda, 2009). The pulse shapes are represented by their binary replacement schemes (Lescop et al., 2010) where open squares account for chemical shift and J-coupling evolution during the pulse duration, while filled squares indicate the time for which the effective spin rotation of either 90° or 180° takes place. For ^{1}H-^{13}C SOFAST-TROSY, EBURP-2 pulse shapes were chosen for the ^{1}H 90° pulses, in order to allow correct tuning of the heteronuclear transfer delays in presence of (relatively) long band-selective pulses of typically a few milliseconds and J_{CH} coupling constants ranging from 125 to 200 Hz. In addition, the sequence of **Fig. 3C** includes the option of CT ^{13}C frequency editing in t_1 which is of interest for ^{1}H-^{13}C spin systems in uniformly ^{13}C-labeled proteins or nucleic acids.

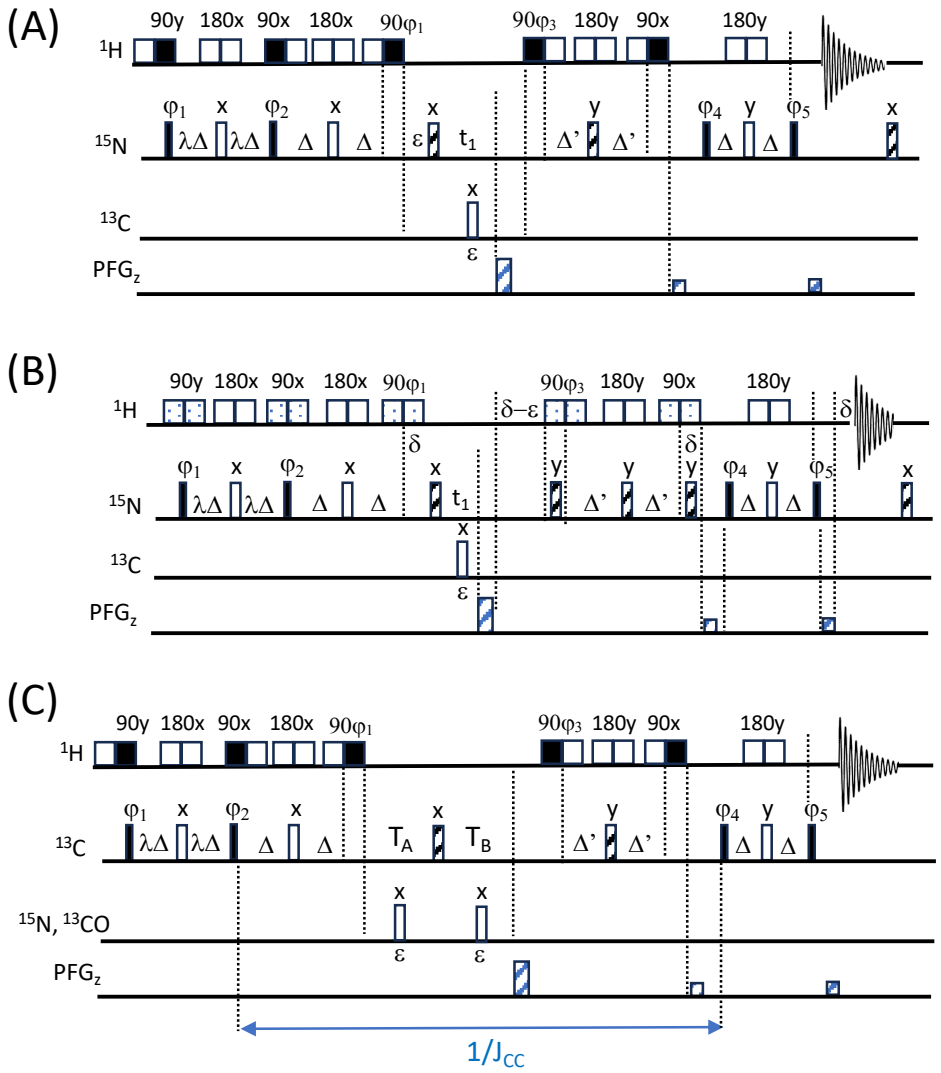

Figure 3. SOFAST-TROSY pulse sequences. (A and B) ^{1}H-^{15}N SOFAST-TROSY. Band-selective ^{1}H pulses are applied with EBURP-2 (90°) (Geen and Freeman, 1991) **and REBURP (180°)** (Geen and Freeman, 1991) **(sequence A) or PC9 (90°)** (Kupce and Freeman, 1993) **and RE-BURP (180°) shapes (sequence B), while broad-band ^{15}N pulses are performed using broad-band UREV2** (Manu et al., 2023) **(open bars) and BIP** (Smith et al., 2001) **(dashed bars) pulse shapes. The transfer delays Δ are adjusted to $\Delta=1/(4J_{NH})$ (with Δ' slightly shorter). The initial phase settings are: φ_1=x, φ_2=x, φ_3=y, φ_4=x, and φ_5=y. Phase cycling and quadrature detection is performed as described in figure 1. (C) ^{1}H-^{13}C SOFAST-TROSY. Band-selective 90° and 180° ^{1}H pulses are applied with E-BURP2 and REBURP profiles. For conventional ^{13}C editing $T_A=\varepsilon$ and $T_B = t_1+\varepsilon$, while for CT-editing, $T_A= 1/(2J_{CC})-2\Delta-t_1/2$ and $T_B= 1/(2J_{CC})-2\Delta'+t_1/2$. The initial phase settings are: φ_1=x, φ_2=x, φ_3=y, φ_4=x, and φ_5=-y. Phase cycling and quadrature detection is performed as described in Fig. 1.**

First, we applied the ^{1}H-^{15}N SOFAST-TROSY experiment to uniformly ^{13}C/^{15}N- and ^{13}C/^{15}N/^{2}H- labelled samples of ubiquitin (25°C). For both samples, the pulse sequence of **Fig. 3B** was preferred, because of a slightly higher sensitivity at short recycle delays. **Figure 4A** illustrates the spectral quality (line shapes) obtained. The performance in terms of experimental sensitivity can be appreciated from the graphs of **Figs. 4B** (^{13}C/^{15}N/^{2}H-ubiquitin) and **4C** (^{13}C/^{15}N-ubiquitin).

We recorded ^{1}H-^{15}N SOFAST-TROSY spectra for different recycle delays (d_{rc}) and flip angles β optimized for the structured parts of the protein, and compared them to conventional BEST-TROSY (Favier and Brutscher, 2011), and WFB-TROSY (Loria et al., 1999) pulse sequences. The BEST-TROSY data were taken as a reference, and the intensity ratios of SOFAST-TROSY and WFB-TROSY with respect to this reference are plotted as red and black bars, respectively. In the case of the perdeuterated ubiquitin sample, BEST-TROSY and WFB-TROSY perform about equally well, and average sensitivity gains of 25% to 50%, depending on the chosen inter-scan delay, are observed for SOFAST-TROSY. In the case of a fully protonated ubiquitin sample, the situation is quite different. The intensity of individual correlation peaks increases by up to 8-fold when replacing a WFB-TROSY with a BEST-TROSY sequence at very short recycle delays, while only a minor further improvement (~10%) is achieved by SOFAST-TROSY. This observation can be rationalized by the fact that LRE reduces the effective longitudinal ^{1}H relaxation in BEST-TROSY and SOFAST-TROSY to less than 200 ms, bringing T_1 close to T_{rec}. The observed sensitivity increase of < 15% (depending on the specific amide site) is thus again in good agreement with the theoretical expectation for $T_{rec}/T_1 \approx 1$ (**Fig. 1C**).

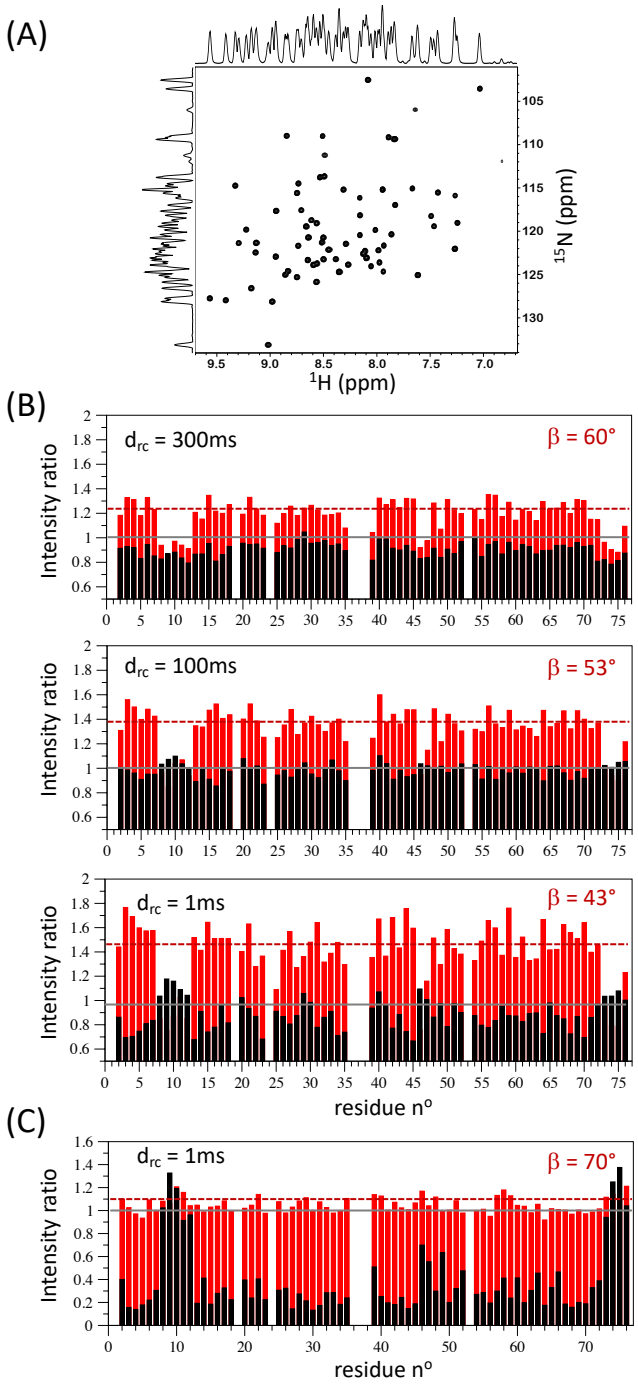

Figure 4. ^{1}H-^{15}N SOFAST-TROSY data of ubiquitin. (A) ^{1}H-^{15}N spectrum recorded at 600 MHz on a uniformly ^{13}C/^{15}N labelled sample of ubiquitin at 25°C with t_{acq}=70 ms, d_{rc} =1 ms and β=70°. (B) Intensity ratios measured for a perdeuterated and ^{13}C/^{15}N labelled sample of ubiquitin at 25°C (950 MHz) with SOFAST-TROSY/BEST-TROSY (red bars) and WFB-TROSY/BEST-TROSY (black bars). The results obtained for different inter-scan delays and experimentally optimized flip angles are shown. (C) Similar data but recorded on a fully protonated ^{13}C/^{15}N labelled sample of ubiquitin and a single inter-scan delay d_{rc} =1 ms.

Figure 5 shows some further applications of the SOFAST-TROSY experiment to molecular systems of different size and nature, with all spectra recorded without any additional recycle delay. The first example is SiR (Sibille et al., 2005), a protein of 18 kDa uniformly enriched in ^{13}C and ^{15}N, and partially deuterated (~60%). ^{1}H-^{15}N spectra were recorded with the pulse sequence of **Fig. 3B**, and a flip angle $\beta \approx 60°$ was found to provide the highest average experimental sensitivity. Compared to an experiment recorded with a 90° excitation flip angle, a sensitivity increase of ~20% was observed (**Fig. 5A**). The remaining applications concern ^{1}H-^{13}C correlation spectra of the aromatic side chains in lysozyme, a 14 kDa protein at natural ^{13}C abundance (**Fig. 5B**), a small RNA hairpin with uniform ^{13}C,^{15}N labelling of U and G nucleotides (**Fig. 5C**) (Rennella et al., 2017), and finally the antibiotic kamamycine, an aminoglycoside composed of 3 sugar units (**Fig. 5D**). For these ^{1}H-^{13}C correlation experiments the sequence of **Fig. 3C** was employed with standard (non-CT) ^{13}C editing for the 2 natural abundance samples, and with CT ^{13}C editing for the uniformly ^{13}C-labelled RNA hairpin. In all 3 cases, a nominal flip excitation angle of 60°-70° was found to be optimal in terms of (average) experimental sensitivity. The sensitivity gain with respect to a $\beta \approx 90°$ reference spectrum, indicative of the longitudinal relaxation times of the ^{1}H and ^{13}C (^{15}N) spins, is different for each of the investigated molecular systems with significant variations observed from one nuclear site to the other.

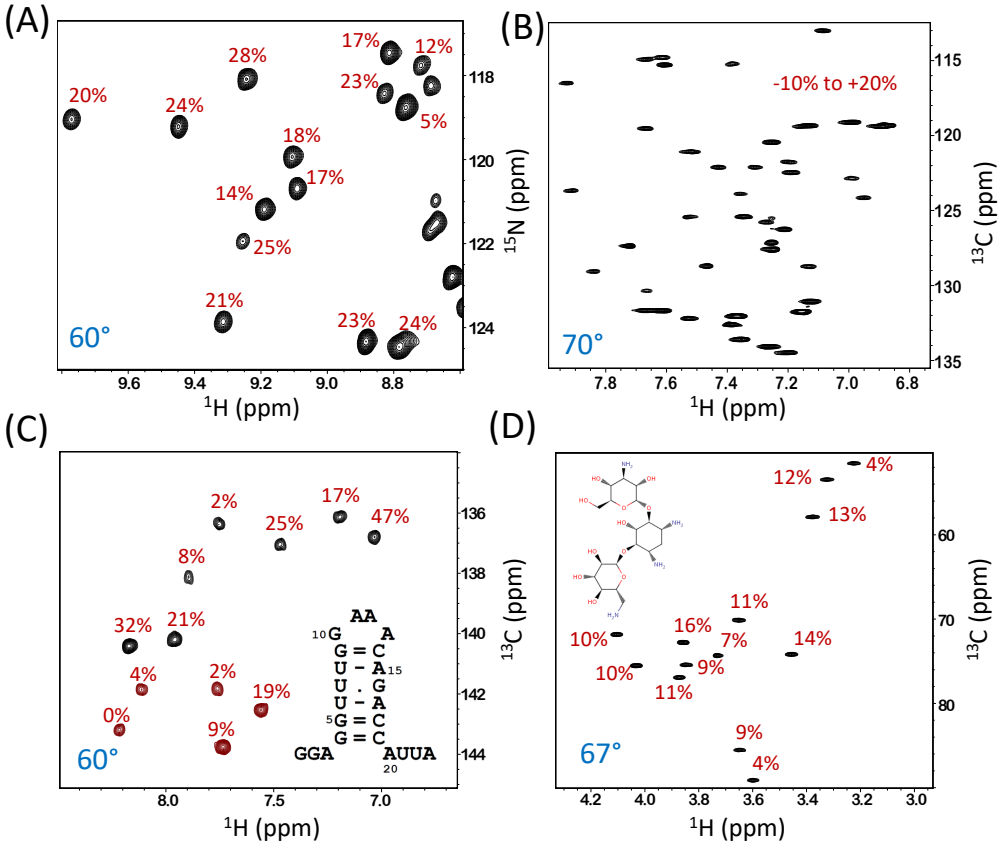

Figure 5. SOFAST-TROSY spectra of different samples, all recorded at 600 or 700 MHz (^{1}H frequency) with an inter-scan delay d_{rc} =1 ms. (A) Small part of ^{1}H-^{15}N spectrum of ^{13}C/^{15}N/^{2}H-labeled SiR (18 kDa, deuteration level ~60%, 30°C, t_{acq} = 70 ms). (B) Aromatic ^{1}H-^{13}C lysozyme spectrum at natural ^{13}C abundance and high sample concentration (2 mM) recorded at 40°C (t_{acq}=100 ms). (C) ^{1}H-^{13}C CT spectrum of 23-nucleotide RNA hairpin with uniformly ^{13}C/^{15}N-labeled G,U nucleotides (25°C, t_{acq}=100 ms). Positive peaks (black contours) are from G, while negative peaks (red) originate from U nucleotides. (D) ^{1}H-^{13}C spectrum of the antibiotic kanamycine at natural ^{13}C abundance and high sample concentration (~10 mM) recorded at 30°C (t_{acq}=100 ms). The numbers (in red) indicate the NMR signal ratio between data recorded with the optimised flip angle (indicated in blue) compared to a data set recorded under identical conditions but with β=90°.

5 Conclusions

We have introduced the PRESERVE pulse sequence element which allows variable flip-angle adjustment in 2D ^{1}H-^{15}N and ^{1}H-^{13}C TROSY-type correlation experiments. Compatible with both hard-pulse-based TROSY versions and shaped-pulse BEST-type implementations, PRESERVE enables versatile applications. PRESERVE-TROSY and SOFAST-TROSY experiments stand out among the wealth of available solution NMR experiments by exploiting a remarkable array of up to 9 parallel polarization-coherence transfer pathways in Cartesian spin operator space. These experiments thus exemplify the remarkable flexibility of nuclear spin manipulations achievable through the design and optimization of NMR pulse sequences. Our focus has been on the theoretical elucidation and experimental realization of the PRESERVE concept. By employing a minimal 2-step phase cycle, clean ^{1}H-^{15}N and ^{1}H-^{13}C correlation spectra can be acquired in short experimental time, making these experiments in principle suitable for a broad range of molecular systems possessing H-N or H-C spin systems. Beyond their conceptual elegance, PRESERVE-TROSY and SOFAST-TROSY provide valuable additions to the NMR toolbox. Whether PRESERVE-TROSY and SOFAST-TROSY experiments yield sensitivity enhancements under fast-pulsing conditions is contingent upon various factors, such as molecular size, isotope labelling scheme, and magnetic field strength, determining the relaxation properties of the sample under investigation. As a rule of thumb, these experiments will be particularly beneficial for molecular systems characterized by prolonged spin-lattice relaxation times of both correlated nuclear spins. Extension of the PRESERVE-TROSY concept to higher dimensional triple-resonance correlation experiments is possible and currently under development in our laboratory.

Code and data availability

The presented pulse sequences are provided as Supplementary information material, and they will also be included in the NMRlib package that is freely available at the following URL: http://www.ibs.fr/nmrlib. NMR data/spectra have been deposited and can be accessed through the following link: https://doi.org/10.5281/zenodo.11447367

Competing interests

BB is Associate Editor with MR

Acknowledgements

The author thanks Adrien Favier (IBS) and Paul Schanda (ISTA, Austria) for stimulating discussions. Financial support from the Agence Nationale de la Recherche (grant no. ANR-22-CE11-0011-01) and from the IR INFRANALYTICS (FR2054) is gratefully acknowledged. This work used the platforms of the Grenoble Instruct-ERIC centre (ISBG ; UAR 3518 CNRS-CEA-UGA-EMBL) within the Grenoble Partnership for Structural Biology (PSB), supported by FRISBI (ANR-10-INBS-0005-02) and GRAL, financed within the University Grenoble Alpes graduate school (Ecoles Universitaires de Recherche) CBH-EUR-GS (ANR-17-EURE-0003). IBS acknowledges integration into the Interdisciplinary Research Institute of Grenoble (IRIG, CEA).

References

Brutscher, B.: Principles and applications of cross-correlated relaxation in biomolecules, Concepts Magn. Reson., 12, 207–229, https://doi.org/10.1002/1099-0534(2000)12:4<207::AID-CMR3>3.0.CO;2-C, 2000.

Brutscher, B. and Solyom, Z.: Polarization-enhanced Fast-pulsing Techniques, in: Fast NMR data acquisition, 1–48, https://doi.org/10.1039/9781782628361-00001, 2017.

Brutscher, B., Boisbouvier, J., Pardi, A., Marion, D., and Simorre, J.-P.: Improved Sensitivity and Resolution in 1H− 13C NMR Experiments of RNA, J. Am. Chem. Soc., 120, 11845–11851, https://doi.org/10.1021/ja982853l, 1998.

Ernst, R. R. and Anderson, W.: Application of Fourier Transform Spectroscopy to Magnetic Resonance, Rev. Sci. Instrum., 37, 93, https://doi.org/10.1063/1.1719961, 1966.

Farjon, J., Boisbouvier, J., Schanda, P., Pardi, A., Simorre, J.-P., and Brutscher, B.: Longitudinal-relaxation-enhanced NMR experiments for the study of nucleic acids in solution., J. Am. Chem. Soc., 131, 8571–7, https://doi.org/10.1021/ja901633y, 2009.

Favier, A. and Brutscher, B.: Recovering lost magnetization: polarization enhancement in biomolecular NMR., J. Biomol. NMR, 49, 9–15, https://doi.org/10.1007/s10858-010-9461-5, 2011.

Gal, M., Schanda, P., Brutscher, B., and Frydman, L.: UltraSOFAST HMQC NMR and the repetitive acquisition of 2D protein spectra at Hz rates., J. Am. Chem. Soc., 129, 1372–1377, https://doi.org/10.1021/ja066915g, 2007.

Geen, H. and Freeman, R. A. Y.: Band-Selective Radiofrequency Pulses, J. Magn. Reson., 93, 93–141, https://doi.org/10.1016/0022-2364(91)90034-Q, 1991.

Goldman, M.: Interference effects in the relaxation of a pair of unlike spin-1/2 nuclei, J. Magn. Reson., 60, 437–452, https://doi.org/10.1016/0022-2364(84)90055-6, 1984.

Grzesiek, S. and Bax, A.: The Importance of Not Saturating H2O in Protein NMR - Application to Sensitivity Enhancement and Noe Measurements, J., 115, 12593–12594, https://doi.org/10.1021/ja00079a052, 1993.

Kay, L. E., Xu, G. Y., and Yamazaki, T.: Enhanced-Sensitivity Triple-Resonance Spectroscopy with Minimal H2O Saturation, https://doi.org/10.1006/jmra.1994.1145, 1994.

Kern, T., Schanda, P., and Brutscher, B.: Sensitivity-enhanced IPAP-SOFAST-HMQC for fast-pulsing 2D NMR with reduced radiofrequency load., J. Magn. Reson., 190, 333–338, https://doi.org/10.1016/j.jmr.2007.11.015, 2008.

Koos, M. R. M. and Luy, B.: Polarization recovery during ASAP and SOFAST/ALSOFAST-type experiments, J. Magn. Reson., 300, 61–75, https://doi.org/10.1016/j.jmr.2018.12.014, 2019.

Kupce, E. and Freeman, R.: Polychromatic Selective Pulses, J. Magn. Reson. A, 102, 122–126, 1993.

Lescop, E., Kern, T., and Brutscher, B.: Guidelines for the use of band-selective radiofrequency pulses in hetero-nuclear NMR: example of longitudinal-relaxation-enhanced BEST-type 1H-15N correlation experiments, J. Magn. Reson., 203, 190–8, https://doi.org/10.1016/j.jmr.2009.12.001, 2010.

Levitt, M. H.: The Signs of Frequencies and Phases in NMR, J. Magn. Reson., 126, 164–182, https://doi.org/10.1006/jmre.1997.1161, 1997.

Levitt, M. H. and Johannessen, O. G.: Signs of Frequencies and Phases in NMR: The Role of Radiofrequency Mixing, J. Magn. Reson., 142, 190–194, https://doi.org/10.1006/jmre.1999.1929, 2000.

Loria, J. P., Rance, M., and Palmer, A. G.: Transverse-Relaxation-Optimized (TROSY) Gradient-Enhanced Triple-Resonance NMR Spectroscopy, J. Magn. Reson., 184, 180–184, https://doi.org/10.1006/jmre.1999.1891, 1999.

Manu, V. S., Olivieri, C., and Veglia, G.: AI-designed NMR spectroscopy RF pulses for fast acquisition at high and ultra-high magnetic fields, Nat. Commun., 14, 1–11, https://doi.org/10.1038/s41467-023-39581-4, 2023.

Mueller, L.: Alternate HMQC experiments for recording HN and HC-correlation spectra in proteins at high throughput, J. Biomol. NMR, 42, 129–137, https://doi.org/10.1007/s10858-008-9270-2, 2008.

Nagy, T. M., Kövér, K. E., and Sørensen, O. W.: NORD: NO Relaxation Delay NMR Spectroscopy, Angew. Chemie - Int. Ed., 60, 13587–13590, https://doi.org/10.1002/anie.202102487, 2021.

Palmer, A. G., Cavanagh, J., Byrd, R. A., and Rance, M.: Sensitivity improvement in three-dimensional heteronuclear correlation NMR spectroscopy, J. Magn. Reson., 96, 416–424, https://doi.org/10.1016/0022-2364(92)90097-Q, 1992.

Pervushin, K., Riek, R., Wider, G., and Wüthrich, K.: Attenuated T2 relaxation by mutual cancellation of dipole-dipole coupling and chemical shift anisotropy indicates an avenue to NMR structures of very large biological macromolecules in solution, Proc. Natl. Acad. Sci. U. S. A., 94, 12366–12371, https://doi.org/10.1073/pnas.94.23.12366, 1997.

Pervushin, K., Riek, R., Wider, G., and Wüthrich, K.: Transverse relaxation-optimized spectroscopy (TROSY) for NMR studies of aromatic spin systems in 13C-labeled proteins, J. Am. Chem. Soc., 120, 6394–6400, https://doi.org/10.1021/ja980742g, 1998a.

Pervushin, K., Vo, B., and Eletsky, A.: Longitudinal 1H Relaxation Optimization in TROSY NMR Spectroscopy, J. Am. Chem. Soc., 124, 12898–12902, https://pubs.acs.org/doi/10.1021/ja027149q, 2002.

Pervushin, K. V., Wider, G., and Wüthrich, K.: Single-transition-to-single-transition polarization transfer (ST2-PT) in [15N,1H]-TROSY, J. Biomol. NMR, 12, 345–348, https://doi.org/10.1023/A:1008268930690, 1998b.

Rennella, E., Sára, T. S., Juen, M., Wunderlich, C., Imbert, L., Solyom, Z., Favier, A., Ayala, I., Weinhäupl, K., Schanda, P., Konrat, R., Kreutz, C., and Brutscher, B.: RNA binding and chaperone activity of the E. coli cold-shock protein CspA,

Nucleic Acids Res., 1–14, https://doi.org/10.1093/nar/gkx044, 2017.

Schanda, P.: Fast-pulsing longitudinal relaxation optimized techniques: Enriching the toolbox of fast biomolecular NMR spectroscopy, Prog. Nucl. Magn. Reson. Spectrosc., 55, 238–265, https://doi.org/10.1016/j.pnmrs.2009.05.002, 2009.

Schanda, P. and Brutscher, B.: Very fast two-dimensional NMR spectroscopy for real-time investigation of dynamic events in proteins on the time scale of seconds., J. Am. Chem. Soc., 127, 8014–8015, https://doi.org/10.1021/ja051306e, 2005.

Schanda, P., Kupce, E., and Brutscher, B.: SOFAST-HMQC experiments for recording two-dimensional heteronuclear correlation spectra of proteins within a few seconds., J. Biomol. NMR, 33, 199–211, https://doi.org/10.1007/s10858-005-4425-x, 2005.

Schanda, P., Van Melckebeke, H., and Brutscher, B.: Speeding up three-dimensional protein NMR experiments to a few minutes., J. Am. Chem. Soc., 128, 9042–9043, https://doi.org/10.1021/ja062025p, 2006.

Schulte-Herbrüggen, T. and Sorensen, O. W.: Clean TROSY: compensation for relaxation-induced artifacts., J. Magn. Reson., 144, 123–8, https://doi.org/10.1006/jmre.2000.2020, 2000.

Sibille, N., Blackledge, M., Brutscher, B., Covès, J., and Bersch, B.: Solution structure of the sulfite reductase flavodoxin-like domain from Escherichia coli, Biochemistry, 44, https://doi.org/10.1021/bi050437p, 2005.

Smith, M. A., Hu, H., and Shaka, A. J.: Improved Broadband Inversion Performance for NMR in Liquids, J. Magn. Reson., 151, 269–283, https://doi.org/10.1006/jmre.2001.2364, 2001.

Solyom, Z., Schwarten, M., Geist, L., Konrat, R., Willbold, D., and Brutscher, B.: BEST-TROSY experiments for time-efficient sequential resonance assignment of large disordered proteins., J. Biomol. NMR, 55, 311–21, https://doi.org/10.1007/s10858-013-9715-0, 2013.

Sørensen, M. D., Meissner, A., and Sørensen, O. W.: Spin-state-selective coherence transfer via intermediate states of two-spin coherence in IS spin systems : Application to E . COSY-type measurement of J coupling constants, J. Biomol. NMR, 10, 181–186, https://doi.org/10.1023/A:1018323913680, 1997.

Weigelt, J.: Single Scan, Sensitivity- and Gradient-Enhanced TROSY for Multidimensional NMR Experiments, J. Am. Chem. Soc., 120, 10778–10779, https://doi.org/10.1021/ja982649y, 1998.

Zuiderweg, E. R. P. and Rousaki, A.: Gradient-enhanced TROSY described with Cartesian product operators, Concepts Magn. Reson., 38 A, 280–288, https://doi.org/10.1002/cmr.a.20228, 2011.